Available online at www.sciencedirect.com
SCIENCE DIRECT®
Journal of Photochemistry and Photobiology A: Chemistry 164 (2004) 159–166
Journal of Photochemistry and Photobiology A:Chemistry
www.elsevier.com/locate/jphotochem

Hydrothermal preparation of porous nano-crystalline TiO_2 electrodes for flexible solar cells

Dongshe Zhang, Tsukasa Yoshida*, Ken Furuta, Hideki Minoura

Environmental and Renewable Energy Systems (ERES) Division, Graduate School of Engineering, Gifu University, 1-1 Yanagido, Gifu 501-1193, Japan

Received 2 September 2003; received in revised form 26 November 2003; accepted 26 November 2003

Abstract

Mechanically stable porous thick film electrodes of nano-crystalline TiO_2 have been prepared at a low temperature from mixed pastes of nano-crystalline TiO_2 particles and Ti-monomers such as $TiCl_4$, $TiOSO_4$, and Ti-tetraisopropoxide, which are converted into crystalline rutile or anatase TiO_2 by hydrothermal treatment at the solid/gas interface and chemically connect the TiO_2 particles. Rigid and flexible dye-sensitized solar cells (DSSCs) employing these materials achieved conversion efficiencies as high as 4.2 and 2.5% under AM 1.5 simulated sunlight (1 sun), respectively. These electrodes exhibited a linear increase of I_{sc} against the light intensity beyond 2 sun level, suggesting an ideal porous structure of the film. However, imperfectness of the low-temperature materials has been indicated from the significant improvement of the cell efficiencies by post-heat treatment of the films at 450 °C. Incomplete necking of the particles as well as the presence of residual organics are thought as the reasons which limit the efficiencies of the low-temperature materials.

Keywords: Flexible solar cells; Hydrothermal crystallization; Nano-crystalline TiO_2 films; Dye sensitization

1. Introduction

Flexible dye-sensitized solar cells (DSSCs) and its counterpart of other flexible photovoltaic devices using transparent conductive plastic substrates have attracted a number of interests recently [1–8] because it would reduce not only the weight but also the cost of the device. Behind it, low-temperature preparation of efficient porous nanoparticulate thick semiconductor film electrodes is a key issue [1–15]. Although the conventional preparation method using organic additives for crack-free coating and high-temperature, thermal–chemical calcination can achieve good interconnection between particles as well as good adherence of the films to the substrates, thus yielding porous nano-crystalline electrodes with an optimum microstructure for photosensitization [16–18]; the same method can not be employed for plastic substrates. Recently, some efforts have been made to develop methods compatible with plastic substrates such as chemical deposition [9], sintering of colloids at a low temperature [1,4,10,11], mechanical compression of crystalline particles [2,13], and electrophoretical deposition [6,15]. However, electrochemical impedance spectroscopy study has revealed a larger inherent resistance of such films than that of the conventional material [4b]. Time- and frequency-resolved photoelectrochemical measurements have also shown that the diffusion coefficient and the lifetime of the electrons are lower [9a,11], resulting in the lower photocurrent, fill factor, and conversion efficiency of the cells. It is therefore important to develop low-temperature methods with respect to the interparticulate connectivity and the adherence of the film to the conducting substrate, in order to improve the performance of the cells.

Recently, we have developed a novel low-temperature chemical method to prepare porous TiO_2 thin films based on hydrothermal crystallization at the solid/gas interface [3,14]. Titanium monomers such as $TiCl_4$, $TiOSO_4$, and Ti(IV)-tetraisopropoxide (TTIP) mixed with nano-crystalline TiO_2 powder are hydrolyzed and crystallize into TiO_2 when they are treated by hot steam. The newly formed crystalline TiO_2 acts as "interconnects" of the TiO_2 particles as well as that between the film and the substrate. The resultant films are mechanically stable, strongly adherent to the substrate, and present high performances when they are used as photoelectrodes.

The present paper aims to update the current status of this novel low-temperature method for realization of

* Corresponding author. Tel.: +81-58-293-2594; fax: +81-58-293-2587.
E-mail address: yoshida@apchem.gifu-u.ac.jp (T. Yoshida).

1010-6030/$ – see front matter © 2004 Elsevier B.V. All rights reserved.
doi:10.1016/j.jphotochem.2003.11.018

efficient flexible plastic DSSCs. Details of the synthesis, structural, chemical, and photoelectrochemical characterizations as well as the effect of post-heat treatment are reported. Through these investigations, the usefulness of the hydrothermal treatment for the interparticulate connection has been proven. At the same time, however, the limitation under the presently adopted preparation conditions has been elucidated when the low-temperature cell was compared with the cell employing a film subjected to a post-heat treatment which in fact presented a significantly better performance. Strategies to improve the performance of the plastic cells are discussed based on the present results.

2. Experimental details

2.1. Preparation of porous nano-crystalline thick TiO_2 films

Pure $TiCl_4$ (Kishida) was dropwisely added into ice-cold distilled water under vigorous stirring to obtain 1 M stock solution. The solution could be stored for more than 1 year in a refrigerator without precipitation. 1 M aqueous $TiOSO_4 \cdot xH_2O$ solution was prepared by dissolving into distilled water at room temperature. This solution also remained stable for more than 1 year in a refrigerator. Ti(IV)-tetraisopropoxide (TTIP) was added into dry ethanol at 1 M. The water content in ethanol was less than 0.05% as controlled by Karl Fischer titration. In a closed bottle, it could be stored for about 50 days without precipitation at room temperature. After 50 days, however, some white particles were produced probably due to hydrolysis of TTIP. Fresh solutions without precipitates were only used for experiments.

Nano-crystalline TiO_2 powder (0.8 g; Degussa P25, 30% rutile, and 70% anatase; BET surface area, 55 $m^2\ g^{-1}$; particle size, 25 nm) was added to 3.2 g of the 1 M $TiCl_4$ or $TiOSO_4$ aqueous solutions, and ground in an agate mortar for about 2 h to get a viscous paste. Since TTIP solution is highly unstable in air, a mixture of 0.8 g P25 and 2.8 g 1 M TTIP solution was prepared in a closed bottle and stirred by a magnetic sitter for 1 day to get a viscous paste. These pastes were coated on a fluorine-doped SnO_2-coated conductive glass (FTO) (Asahi Glass, 10 Ω/□) or an indium tin oxide (ITO)-coated poly(ethylene terephthalate) (PET) film (sheet resistance, ca. 70 Ω) by a glass rod and using Scotch tape as spacers. However, the ITO/PET film substrates could not be used for the pastes with $TiCl_4$ and $TiOSO_4$ precursors because these acidic pastes damaged the ITO layer, while the paste with TTIP could be used for both substrates. After drying in air at room temperature, the coated substrates were put into a Teflon-lined autoclave as shown in Fig. 1. A small amount of distilled water was added at the bottom of the reactor so that the sample is not in direct contact with water but with steam during the reaction. The reactor was placed in an oven at 100 °C for 12 h. After the hydrothermal treatment, the films were taken out, rinsed with water, and dried in an oven at 100 °C for 1 h. The resulting film thickness was typically 10 μm, but could be easily controlled by changing the thickness of the spacer. A film thickness up to 18 μm has been achieved by one coating, without causing any problems in the mechanical stability of the film. In order to confirm the effect of the hydrothermal treatment, a sample without hydrothermal treatment was also prepared. A film was prepared by coating the paste with TTIP precursor and simply drying at 100 °C in an oven for a control experiment. The hydrothermally-treated film prepared on an FTO glass substrate has also been subjected to a heat treatment at 450 °C for 30 min to study the effect of post-annealing.

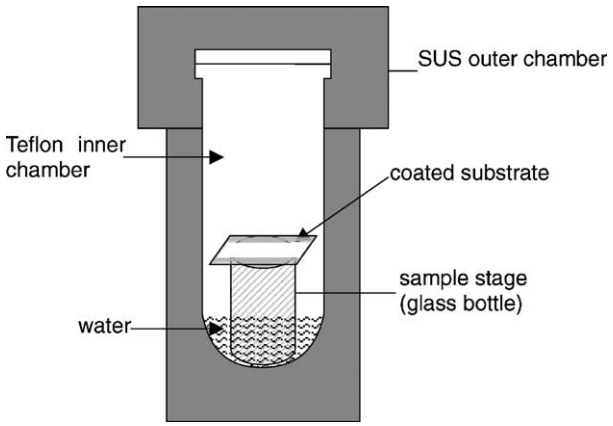

Fig. 1. Experimental set-up for hydrothermal treatment of the films.

2.2. Physico-chemical characterization

The film thickness was measured by using a Kosaka Lab. SE-2300 surface profilometer. The surface morphology of the films was observed on a Topcon ABT-150FS scanning electron microscope (SEM). The crystallization of the Ti-monomers into TiO_2 during the hydrothermal reaction has been investigated by measuring X-ray diffraction patterns (XRD) of the films prepared by drop-coating of the solutions of the Ti-monomers without P25 on a Rigaku RAD-2R using Cu Kα radiation. X-ray photoelectron spectra (XPS) were measured for C 1s signal using a ESCA-3400 spectrometer (Shimadzu) with the Al Kα X-ray line (1486.6 eV) for the hydrothermally-treated film and that subjected to the post-heat treatment. The films were prepared from P25 + TTIP paste for this purpose. The spectra were calibrated for charging of the sample by using Ti 2p peak position (459.5 and 465.2 eV) as the standard which was dominated by the signal arising from the added P25.

2.3. Sensitization of the films and photoelectrochemical measurements

The dry, warm electrodes were immersed in a 0.5 mM ethanol solution of $Ru(II)(dcbpy)_2(NCS)_2$ (dcbpy: 2,2′-

bipyridine-4,4′-dicarboxylic acid) (hereafter called N3) dye overnight at room temperature for sensitization. The dye loading was determined by desorbing the dye from the sensitized film of a known area in a measured volume of ethanol containing NaOH, and measuring its absorption spectrum.

Photocurrent-voltage measurements were made in a two-electrode sandwich configuration. The dye-sensitized electrode with an effective area of ca. 0.2 cm^2 was employed as a working electrode and a platinized ITO/PET or FTO glass as a counter electrode. The electrolyte was 3-methoxypropionitrile containing 0.5 M LiI, 0.05 M I_2, and 0.5 M *tert*-butylpyridine. Bunko–Keiki CEP-2000 system provided means of photocurrent-voltage measurements under illumination with an AM 1.5 simulated sunlight (100 mW cm^{-2}) as well as the measurements of photocurrent action spectra under monochromatic light illumination with a constant photon number (10^{16} cm^{-2} s^{-1}). The conversion efficiencies reported here were from yields that were not corrected for losses due to light absorption and reflection by the substrates. Visible light generated from a 500 W Xe arc lamp (Ushio) equipped with a $\lambda > 420$ nm longpass and an IR cutoff filters was also used as the light source for the purpose of studying the linearity of photocurrent to the light intensity. Use of neutral density (ND) filters could vary the light intensity without changing the spectrum for this light source. The number of photons for this light source at the highest light intensity used in this measurement (104.2 mW cm^{-2}) is equivalent to that of 2.2 suns for the AM 1.5 spectrum in the range useful for the N3 dye (between 400 and 700 nm).

3. Results and discussion

3.1. Hydrothermal crystallization at solid/gas interface

Hydrothermal technique is a popular method for preparation of ceramic powders. Usually, the reaction is carried out in the solution phase, where the metastable precursors are hydrolyzed and converted into crystalline particles. Such a reaction is therefore extensively employed and investigated for the synthesis of monodispersed nano-crystalline powders of metal oxides used in DSSCs such as TiO_2 [16c,19,20]. However, the gas phase of such reaction environment has been rarely regarded as a useful reaction medium. Interestingly, we have found that similar hydrothermal crystallization is achieved at the solid/gas interface when the gas phase is saturated with water. This reaction, therefore, allows direct conversion of solid precursor into crystalline films [3,14]. Several Ti-monomers were tested for their conversion into crystalline TiO_2. Fig. 2(1) compares XRD patterns for the films prepared by spreading the solutions of the Ti-monomers on FTO glass substrates which are either simply dried under air at room temperature or exposed to steam at 100 °C for 12 h. When $TiCl_4$ aqueous solution is

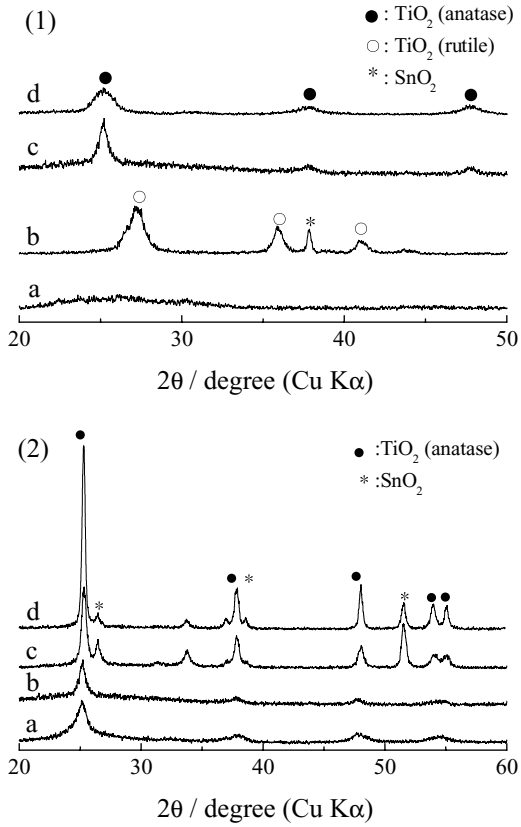

Fig. 2. (1) XRD patterns of the TiO_2 film prepared from $TiCl_4$ solution by drying in air at room temperature for 12 h (a); the same film after the hydrothermal treatment at 100 °C for 12 h (b); the film prepared from the $TiOSO_4$ solution after the hydrothermal treatment at 100 °C for 12 h (c); and the film prepared from the TTIP solution after the hydrothermal treatment at 100 °C for 12 h (d). (2) XRD patterns of the TiO_2 films prepared from the $TiOSO_4$ solution after hydrothermal treatment for 12 h at 80 (a); 100 (b); 150 (c); and 180 °C (d).

drop-coated and kept at room temperature, it remains amorphous as noticed from the absence of any diffraction peaks (a). The coatings from the aqueous solutions of $TiOSO_4$ and ethanolic solution of TTIP are also not crystallized after drying. However, when they are treated by hot steam, they are selectively crystallized either into rutile ($TiCl_4$ (b)) or anatase ($TiOSO_4$ (c) and TTIP (d)) TiO_2. It should be noted that heating of these samples in a dry-oven at 100 °C or higher temperatures up to 300 °C does not lead to a formation of crystalline materials. This clearly indicates that the hydrothermal crystallization can occur at the solid/gas interface even at a temperature as low as 100 °C. It is evident that the presence of water in the gas phase is very important for this process. Park et al. [21] have also reported formation of highly crystallized ZrO_2-compact thin film by hydrothermal dehydration of amorphous Zr hydroxide film at 200 °C. They did not observe crystallization of ZrO_2 when the raw material was heated in a dry-oven even at a much higher temperature. The phase-selective crystallization of TiO_2 is in agreement with the results of hydrothermal synthesis of TiO_2 powders in solution phase using the same precursors

[20], suggesting that the reactions at the solid/gas interface are similar to those in the solution bulk.

Fig. 2(2) shows XRD patterns for the films prepared from the $TiOSO_4$ precursor which were hydrothermally-treated at different temperatures. It is noticed that formation of crystalline anatase TiO_2 occurs even at a fairly low temperature of 80 °C. The diffraction peaks become sharper and increase their intensity with increasing the temperature, indicating that further crystal growth is indeed possible at slightly elevated temperatures. However, PET film decomposes at temperatures above ca. 130 °C under hydrothermal condition, although it survives 150 °C when it is heated for a short time in a dry-oven. It was also noticed that ITO layer increased its resistance after the hydrothermal treatment, while FTO seemed to be stable. Hydrothermal treatment at temperatures higher than 100 °C was therefore not practical as far as the ITO/PET film substrates are concerned.

3.2. Synthesis of porous TiO_2 thick films

By dispersing nano-crystalline TiO_2 powders such as P25 into these solutions of Ti-monomers, homogeneous pastes can be prepared. In case of aqueous precursors, the mixture can be ground in an agate mortar, because hydrolysis of $TiCl_4$ and $TiOSO_4$ are fairly slow process under ambient conditions. However, the mixed paste with TTIP has to be prepared in a closed bottle, because it quickly decomposes by reacting with water in air. In fact, the raw films prepared by coating of the pastes with $TiCl_4$ and $TiOSO_4$ are quickly dissolved into water, while that with TTIP did not, because the added TTIP is quickly converted into solids upon drying. In case of the mixture with TTIP, overnight stirring by magnetic stirrer yielded adequately homogeneous dispersion of the P25 particles, although we have also tested several other methods to apply higher mechanical stress such as ball milling and ultrasonication. It is supposed that slow chemical disgregation of TiO_2 particles proceeds in ethanol, so that high shear stress is not needed for this mixture. All of the films prepared from these mixed pastes withstand gas phase hydrothermal treatment and the resultant films are strongly adherent to the substrates and do not dissolve to water.

Change of the surface morphology of the film before and after the steam treatment has been observed by SEM for those prepared with the TTIP precursor (Fig. 3). The fresh raw film has a non-porous structure in which particles of P25 are seemingly covered with another amorphous material (a). After the steam treatment, the individual particles become apparent and the film becomes highly porous (b). The average size of particles is ca. 25 nm, which matches that of P25 particles. No cracks are found even in the low magnification image (c), suggesting that the particles are nicely dispersed even in the absence of organic surfactants. In fact, this morphology is very similar to that of the porous nano-crystalline TiO_2 film prepared by the standard high-temperature method [16]. Similar morphological changes were found for the films prepared with the other Ti-monomers in the paste. It

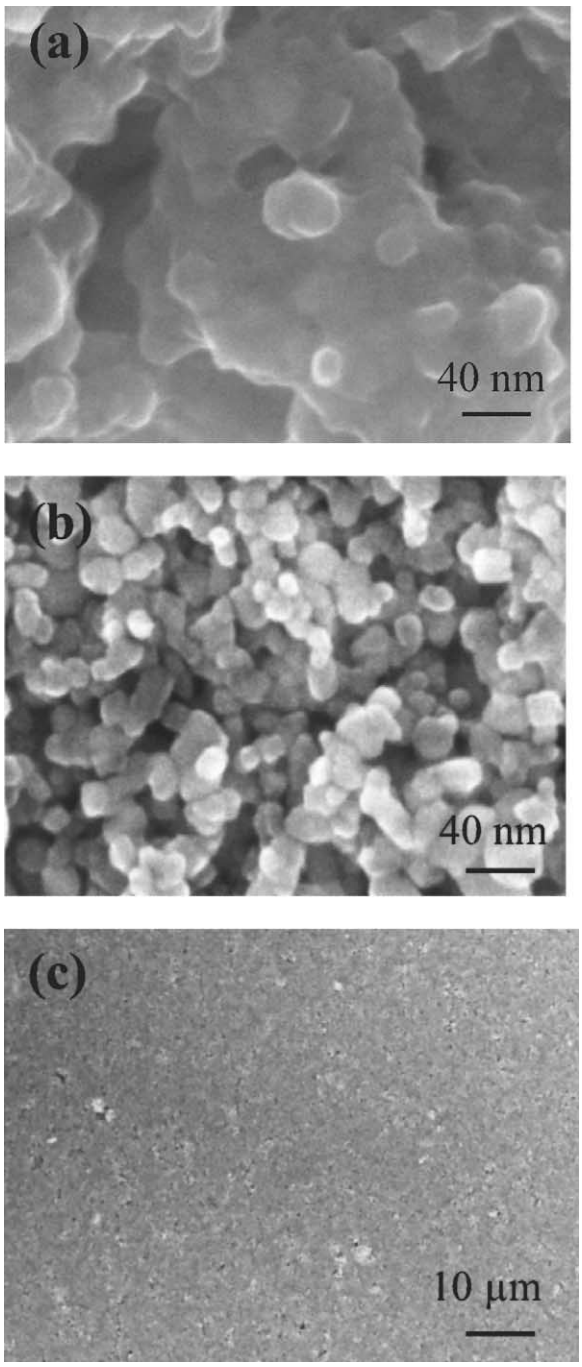

Fig. 3. SEM photographs of the TiO_2 films prepared from the P25 + TTIP-mixed paste before (a) and after (b) the hydrothermal treatment at 100 °C for 12 h; the same as (b) at lower magnification (c).

should also be noted that post-annealing of the film at 450 °C following the hydrothermal preparation did not cause any noticeable change of the film morphology (not shown), indicating that the porous structure is formed already at the stage of the hydrothermal treatment.

According to the information from SEM and XRD, the film formation in the present hydrothermal process can be depicted as Fig. 4. In the raw film, the Ti-monomers added

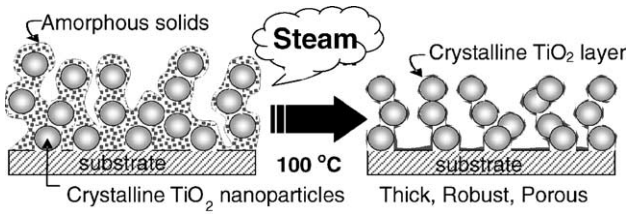

Fig. 4. Schematic representation of the film formation during the hydrothermal crystallization at the gas/solid interface.

in the paste are converted into amorphous solids which surround nano-crystalline TiO_2 particles. During the hydrothermal treatment, the amorphous solids are crystallized into TiO_2 and reduce their volume so that the film becomes porous. Consequently, the added Ti-monomers act just like a "glue" to connect the TiO_2 particles as well as to attach the film to the substrate. The resultant films are therefore mechanically highly stable. A film thickness up to 18 μm could be reached by one coating using a thick spacer, without causing problems in the stability of the film, although the thickness was adjusted to 10 μm in the following experiments. Assuming that the P25 particles are perfect spheres with 25 nm diameter and that crystalline TiO_2 which originate from the added Ti-monomers forms uniform layers around the P25 particles, the expected thickness of the newly formed TiO_2 layer can be calculated. It is as thin as 1.4 nm for the paste composition used in this study. In reality, however, it is supposed that the added Ti-monomers are condensed at the grain boundaries upon drying the paste for necking of the particles. The interparticulate connection with crystalline TiO_2 should also be beneficial in terms of the efficient electron transport through the porous network.

3.3. Dye-sensitization and cell performances

The porous thick films, prepared by the present method, were deeply colored by soaking them into the solution of N3 dye. For comparison, the raw film prepared with TTIP precursor without hydrothermal treatment was also sensitized. The amount of the adsorbed N3 dye per projected film area was checked by desorbing the dyes from the film and measuring Vis absorption spectrum. The values are listed in Table 1. The hydrothermally-treated films have high dye loading exceeding 1×10^{-7} mol cm^{-2} for the film thickness of 10 μm, indicating their high porosity. The raw film can also be colored, although its dye loading goes down to 0.76×10^{-7} mol cm^{-2}, as expected from its less porous structure (Fig. 3(a)).

The sandwich cells fabricated with the sensitized TiO_2 film electrodes exhibited high performances. The cell parameters measured under illumination with AM 1.5 simulated sunlight (100 mW cm^{-2}) are summarized in Table 1. The highest conversion efficiency of 4.2% has been achieved for the cell, employing the film prepared with the $TiCl_4$ precursor, followed by 3.3 and 1.8% of those prepared with the TTIP and $TiOSO_4$ precursors, respectively. The difference of the efficiency arises mainly from that of short circuit photocurrent. The maximum IPCE values (at 520 nm) measured for these cells are 58, 52, and 28%, which follow the order of their efficiencies. The importance of the hydrothermal treatment is obvious, as the cell fabricated with the raw film has a much lower efficiency of 0.4%, although it does work as a solar cell, which is quite surprising on considering the fact that the interparticulate connection in this material is made with amorphous insulating Ti oxide/hydroxide.

In order to realize fabrication of flexible solar cells, the films have to be prepared on plastic substrates. However, the pastes containing $TiCl_4$ and $TiOSO_4$ unfortunately could not be used, because these acidic precursors dissolve the ITO layer, which is the only choice of transparent conducting layer for plastic films. Films could be prepared on the ITO/PET flexible substrates with the paste containing TTIP as it does not damage the ITO layer. However, the sheet resistance of the ITO layer slightly increased from 70 to 90 Ω/□after the hydrothermal treatment. The *I–V* curve measured for the flexible solar cell is shown in Fig. 5. The cell parameters are slightly worse than those obtained with the same film prepared on an FTO glass substrate, achieving an overall energy conversion efficiency of 2.5%. The maximum IPCE value for this cell was 41%.

3.4. Linearity to the light intensity and the effect of post-annealing

Although the conversion efficiencies obtained with the porous TiO_2 films prepared by the hydrothermal method are still not achieving the highest level, one can reach by the

Table 1
Dye loading, maximum IPCE, and the cell parameters of the sandwich cells (effective area, 0.2 cm^2) employing porous nano-crystalline TiO_2 electrodes prepared from different precursors and on different substrates

Precursor	Substrates	Dye loading (10^{-7} mol/cm^2)	IPCE (% at 520 nm)	I_{sc} (mA/cm^2)	V_{oc} (V)	FF	η (%)
$TiCl_4$	FTO	1.5	58	9.4	0.71	0.63	4.2
$TiOSO_4$		1.7	27	3.6	0.70	0.69	1.8
TTIP		1.2	52	7.4	0.72	0.64	3.3
TTIP[a]		0.76	4	0.8	0.68	0.64	0.4
TTIP	ITO/PET	1.1	41	6.1	0.70	0.61	2.5

The cell parameters were measured under illumination with AM 1.5 simulated sunlight (100 mW cm^{-2}).
[a] The electrode without steam treatment.

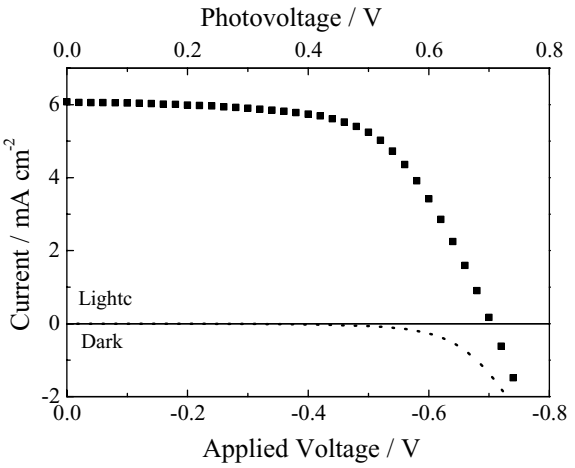

Fig. 5. *I–V* curves of the plastic solar cell prepared on ITO/PET film substrates measured under illumination with AM 1.5 simulated sunlight (100 mW cm^{-2}).

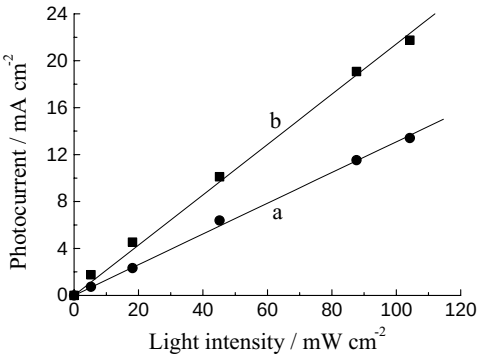

Fig. 6. The linearity of the I_{sc} vs. light intensity measured for the cells employing porous nano-crystalline TiO_2 photoelectrodes prepared by hydrothermal treatment of the P25 + TTIP mixed paste at 100 °C for 12 h (a) and the same film subjected to post-annealing at 450 °C for 30 min (b).

conventional high-temperature methods, one of the favorable characters of the present materials can be found in the fact that they exhibit a linear increase of I_{sc} against the incident light intensity (Fig. 6(a)). In this measurement, a 500 W Xe arc lamp filtered for visible light with a $\lambda > 420$ nm longpass and IR cutoff filter was used as the light source, in order to allow attenuation of light intensity by ND filters without changing the light spectrum. The I_{sc} increases linearly to the light intensity reaching the highest value of 13.4 mA cm^{-2} at 104 mW cm^{-2}. It should be considered that this light source at the highest intensity contains visible light equivalent to that of 2.2 times of sunlight by the number of photons in the range where the dye can absorb, thus proving the current linearity of the present material beyond 2 sun level. The non-linearity of photocurrent against the incident light intensity has been reported as a problem with the porous semiconductor film electrodes prepared by mechanical compression [13a]. Although a high conversion efficiency of 4.5% is achieved under a weak light illumination at 1/10 of sunlight, it dropped to 3% at the 1 sun level due to the non-linearity of photocurrent. Limitation of photocurrent due to the limited transport of electrolyte and/or the increase of electrical resistance of the conducting layer due to its cracking during the mechanical compression at high pressure are supposed as the reasons. By contrast, the cell fabricated with the present material prepared by hydrothermal reaction achieved almost constant conversion efficiencies around 5% over a wide range of light intensity in this measurement (Table 2) owing to the linearity of the photocurrent, although, the absolute value of the conversion efficiency is not to be compared directly because the light source used in this measurement is focused in the visible range. It is, however, evident from these measurements that the present material does not suffer from the limited photocurrent, owing to the ideal porous structure similar to that obtained by the conventional high-temperature sintering method. It is also obvious that the transparent conducting layer cannot be mechanically damaged even in the case of the soft plastic film substrates because the film formation is made by simple coating of the pastes.

A large room of further improvement has been indicated by the fact that post-annealing of the hydrothermally prepared film at 450 °C results in a dramatic improvement of the cell performance. The photocurrent is almost doubled, and the overall conversion efficiency as high as 10% is achieved under illumination with the filtered Xe lamp (Table 2). The linear increase of photocurrent against light intensity has been confirmed also for the sintered electrode, achieving a photocurrent density of 21.8 mA cm^{-2} at the highest intensity (Fig. 6(b)).

Table 2
The cell parameters measured under different light intensities for the cells employing porous nano-crystalline TiO_2 photoelectrodes prepared by hydrothermal treatment of the P25 + TTIP-mixed paste at 100 °C for 12 h, and the same film subjected to post-annealing at 450 °C for 30 min

Light intensity (mW cm^{-2})	Hydrothermal only				Hydrothermal + post-annealing			
	I_{sc} (mA cm^{-2})	V_{oc} (mV)	FF	η (%)	I_{sc} (mA cm^{-2})	V_{oc} (mV)	FF	η (%)
5.26	0.736	446	0.749	4.68	1.75	504	0.614	10.3
18.2	2.33	536	0.681	4.68	4.53	571	0.687	9.79
45.2	6.38	593	0.621	5.19	10.1	635	0.696	9.90
87.7	11.5	650	0.586	5.01	19.1	668	0.651	9.46
104	13.4	682	0.586	5.14	21.8	692	0.666	9.61

A 500 W Xe arc lamp filtered for visible light with a $\lambda > 420$ nm longpass and an IR cutoff filters was used as the light source for these measurements.

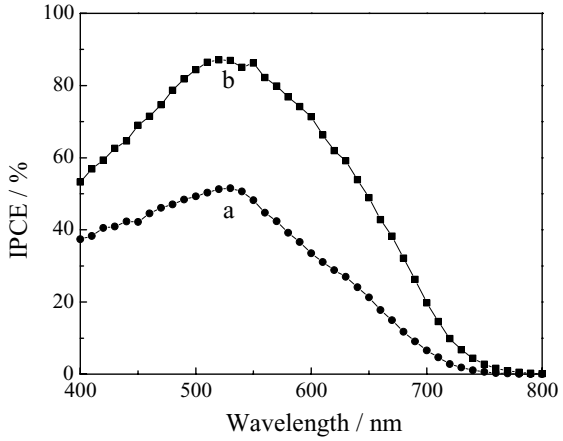

Fig. 7. Photocurrent action spectra measured for the cells employing porous nano-crystalline TiO_2 photoelectrodes prepared by hydrothermal treatment of the P25 + TTIP mixed paste at 100 °C for 12 h (a) and the same film subjected to post-annealing at 450 °C for 30 min (b).

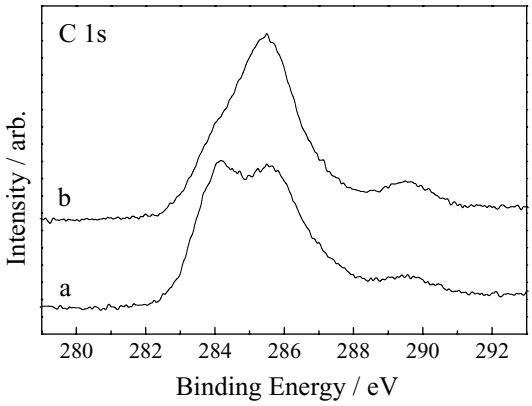

Fig. 8. XPS (C 1s) of the porous nano-crystalline TiO_2 films prepared by hydrothermal treatment of P25 + TTIP-mixed paste at 100 °C for 12 h (a) and the same film subjected to post-annealing at 450 °C for 30 min (b).

Fig. 7 compares the photocurrent action spectra of the cells with and without the post-annealing of the film. The increase of maximum IPCE from 52 to 88% reasons the significant improvement of the cell by post-annealing. A careful observation of the action spectra reveals that the enhancement of the IPCE by post-annealing is pronounced especially at the red end of the spectra. While an enhancement by a factor of about 1.7 is estimated at the maxima, the IPCE values at 700 nm increases by a factor of almost 3. At the wavelength close to dye absorption maximum, photon extinction is completed within the region close to the back contact, so that the photoinjected electrons do not need to travel a long distance. On the other hand, at the red end of the spectra, light penetrates much deeper into the film because of the smaller absorbance of dyes and the smaller degree of light scattering, so that a substantial contribution in photoinjection of electrons is expected from the dye molecules far apart from the back contact. The fact that a much higher portion of the photoinjected electrons lead to current generation in the post annealed material indicates a large improvement in the charge transport property of the TiO_2 layer. It is likely that the necking of the TiO_2 particles is still imperfect in the hydrothermally prepared film, and that the post-annealing of the film at a high temperature completes the connection of the particles. It is however obvious that the annealing at a high temperature is not applicable to the plastic film substrates. It is therefore necessary to develop methods to achieve more complete necking of the TiO_2 particles else than heating.

Another important effect from the post-annealing should exist in the removal of residual organics from the film. X-ray photoelectron spectra of the porous TiO_2 films were measured before and after the heat treatment. The spectra of the films gave major peaks assignable to Ti and O with chemical shifts expected for TiO_2. Additionally, small peaks of C 1s emission were also detected. While the signals of Ti and O remained the same, a change was noticed for the C 1s signal (Fig. 8). The hydrothermally prepared film exhibits two equally large peaks at 284.2 and 285.5 eV and one minor peak at 289.6 eV. After the heat treatment, the double peak changes to a single one at 285.5 eV. It has been reported that the C 1s peaks at 285.5 and 289.6 eV arise from organic contaminants from the ex situ preparation process and/or the transfer process of the sample [22,23]. On the other hand, the peak at 284.2 eV is characteristic for the hydrothermally prepared sample and probably originates from the added TTIP. It is likely that the conversion of TTIP molecules into TiO_2 is incomplete after the hydrothermal treatment and that 2-propanol or its decomposition products partly remain in the film. They are, however, completely removed from the film by heating at a high temperature. It has been indicated that these residual organics on the surface of TiO_2 enhance charge recombination, so that their removal leads to an extension of lifetime of photoinjected electrons, and thus, improvement of charge collection efficiency [24].

4. Conclusion

We have developed a novel low-temperature method to prepare mechanically stable porous thick films of nano-crystalline TiO_2 by employing hydrothermal crystallization at solid/gas interface. Dye-sensitized solar cells employing these TiO_2 film electrodes achieved the highest conversion efficiency of 4.2% under illumination with AM 1.5 simulated sunlight. The conversion efficiency of the plastic cell was somewhat smaller (2.5%) because of the limited choice of the TiO_2 precursor (TTIP) and the limited conductivity of the ITO/PET substrate. The favorable feature of the materials prepared by the present method is the linearity of the photocurrent against the light intensity, probably owing to the ideal porous structure of these materials for unlimited transport of electrolytes. Post-heat

treatment of the hydrothermally prepared porous films at 450 °C significantly improved the efficiency of the cell due to the more complete necking of the particles as well as the removal of residual organics from the film. This indicates the limitation of the hydrothermal method under the present condition; at the same time, however, the presence of large room of further improvement. The following study should therefore concentrate in the optimization of the paste composition and the reaction conditions, as well as the development of post treatments else than heating for the complete conversion of the Ti-monomers into TiO_2. In addition, the flexibility in the choice of the materials should also be the merit of the present method, namely, variety of a core-shell structured composite films may be prepared by combining metal oxide particles else than TiO_2, and metal salts and alkoxides as precursors of other metal oxides [18,25,26].

Acknowledgements

This study is supported by Industrial Technology Research Grant Program in 2003 from New Energy and Industrial Technology Development Organization (NEDO) of Japan (01B64002c) and grant-in-aid for Scientific Research from the Ministry of Education, Culture, Sports, Science and Technology of Japan (15681005).

References

[1] F. Pichot, S. Ferrere, R.J. Pitts, B.A. Gregg, J. Electrochem. Soc. 146 (1999) 4324.
[2] (a) H. Lindström, A. Holmberg, E. Magnusson, L. Malmqvist, A. Hagfeldt, J. Photochem. Photobiol., A 145 (2001) 107;
(b) H. Lindström, A. Holmberg, E. Magnusson, S.-E. Lindquist, L. Malmqvist, A. Hagfeldt, Nano Lett. 1 (2001) 97;
(c) G. Boschloo, H. Lindström, E. Magnusson, A. Holmberg, A. Hagfeldt, J. Photochem. Photobiol., A 148 (2002) 11.
[3] D. Zhang, T. Yoshida, H. Minoura, Adv. Mater. 15 (2003) 814.
[4] (a) M-A. De Paoli, A.F. Nogueira, D.A. Machado, C. Longo, Electrochim. Acta 46 (2001) 4243;
(b) C. Longo, A.F. Nogueira, M-A. De Paoli, H. Cachet, J. Phys. Chem. B 106 (2002) 5925;
(c) C. Longo, J. Freitas, M-A. De Paoli, J. Photochem. Photobiol., A 159 (2003) 33.
[5] R. Gaudiana, J. Macromol. Sci. part A, Pure Appl. Chem. A39 (2002) 1259.
[6] T. Yamada, S. Shiratori, Trans. Mater. Res. Soc. Jpn. 27 (2002) 691.
[7] S.E. Shaheen, C.J. Brabec, N.S. Sariciftci, F. Padinger, T. Fromherz, J.C. Hummelen, Appl. Phys. Lett. 78 (2001) 841.
[8] G. Yu, J. Gao, J.C. Hummelen, F. Wudl, A.J. Heeger, Science 270 (1995) 1789.
[9] (a) N.-G. Park, G. Schlichthörl, J. van de Lagemaat, H.M. Cheong, A. Mascarenhas, A.J. Frank, J. Phys. Chem. B 103 (1999) 3308;
(b) K.-J. Kim, K.D. Benkstein, J. van de Lagemaat, A.J. Frank, Chem. Mater. 14 (2002) 1042.
[10] F. Pichot, J.R. Pitts, B.A. Gregg, Langmuir 16 (2000) 5626.
[11] (a) S. Nakade, S. Kambe, M. Matsuda, Y. Saito, T. Kitamura, Y. Wada, S. Yanagida, Physica E 14 (2002) 210;
(b) S. Nakade, M. Matsuda, S. Kambe, Y. Saito, T. Kitamura, T. Sakata, Y. Wada, H. Mori, S. Yanagida, J. Phys. Chem. B 106 (2002) 10004.
[12] (a) T. Yoshida, K. Terada, D. Schlettwein, T. Oekermann, T. Sugiura, H. Minoura, Adv. Mater. 16 (2000) 1214;
(b) T. Yoshida, H. Minoura, Adv. Mater. 16 (2000) 1219;
(c) T. Yoshida, T. Oekermann, O. Kenji, D. Schlettwein, K. Funabiki, H. Minoura, Electrochemistry 70 (2002) 470.
[13] (a) H. Lindström, E. Magnusson, A. Holmberg, S. Södergren, S.-E Lindquist, A. Hagfeldt, Sol. Energy Mater. Sol. Cells 73 (2002) 91;
(b) K. Keis, E. Magnusson, H. Lindström, S.-E Lindquist, A. Hagfeldt, Sol. Energy Mater. Sol. Cells 73 (2002) 51.
[14] D. Zhang, T. Yoshida, H. Minoura, Chem. Lett. (2002) 874.
[15] T. Miyasaka, Y. Kijitori, T. N. Murakami, M. Kimura, S. Uegusa, Chem. Lett. (2002) 1250.
[16] (a) B. O'Regan, M. Grätzel, Nature 353 (1991) 737;
(b) M.K. Nazeeruddin, A. Kay, I. Rodicio, R. Humphry-Baker, E. Muller, P. Liska, N. Vlachopoulos, M. Grätzel, J. Am. Chem. Soc. 115 (1993) 6382;
(c) C.J. Barbé, F. Arendse, P. Comte, M. Jirousek, F. Lenzmann, V. Shklover, M. Grätzel, J. Am. Ceram. Soc. 80 (1997) 3157.
[17] (a) K. Hara, K. Sayama, Y. Ohga, A. Shinpo, S. Suga, H. Arakawa, Chem. Commun. (2001) 569.;
(b) K. Hara, H. Horiuchi, R. Katoh, L.P. Singh, H. Sugihara, K. Sayama, S. Murata, M. Tachiya, H. Arakawa, J. Phys. Chem. B 106 (2002) 374.
[18] K. Tennakone, G.R.R.A. Kumara, I.R.M. Kottegoda, V.P.S. Perera, Chem. Commun. (1999) 15.
[19] S.T. Aruna, S. Tirosh, A. Zaban, J. Mater. Chem. 10 (2000) 2388.
[20] H. Yin, Y. Wada, T. Kitamura, S. Kambe, S. Murasawa, H. Mori, T. Sakata, S. Yanagida, J. Mater. Chem. 11 (2001) 1694.
[21] S. Park, B.L. Clark, D.A. Keszler, J.P. Bender, J.F. Wager, T.A. Reynolds, G.S. Herman, Science 297 (2002) 65.
[22] G. Liu, W. Jaegermann, J. He, V. Sundström, L. Sun, J. Phys. Chem. B 106 (2002) 5814.
[23] T. Sasaki, Y. Ebina, K. Fukuda, T. Tanaka, M. Harada, M. Watanable, Chem. Mater. 14 (2002) 3524.
[24] T. Oekermann, D. Zhang, T. Yoshida, H. Minoura, J. Phys. Chem. B 108 (2004) 2227.
[25] V. Subramanian, E. Wolf, P.V. Kamat, J. Phys. Chem. B 105 (2001) 10851.
[26] A. Zaban, S.G. Chen, S. Chappel, B.A. Gregg, Chem. Commun. (2000) 2231.